

Design, synthesis, and evaluation of mixed imine–amine pyrrolobenzodiazepine dimers with efficient DNA binding affinity and potent cytotoxicity

Ahmed Kamal,^{a,*} G. Ramesh,^a O. Srinivas,^a P. Ramulu,^a N. Laxman,^a Tasneem Rehana,^a M. Deepak,^b M. S. Achary^b and H. A. Nagarajaram^b

^aBiotransformation Laboratory, Division of Organic Chemistry, Indian Institute of Chemical Technology, Hyderabad 500 007, India

^bLaboratory of Computational Biology and Bioinformatics Facility, Centre for DNA Fingerprinting and Diagnostics, Hyderabad 500 076, India

Received 24 June 2004; revised 21 July 2004; accepted 21 July 2004

Available online 20 August 2004

Abstract—Synthesis of mixed imine–amine pyrrolobenzodiazepine (PBD) dimers that are comprised of DC-81 and secondary amine (N10) of DC-81 subunits tethered to their C8 positions through alkanedioxy linkers (comprised of three and five carbons) is described. These noncross-linking unsymmetrical molecules exhibit significant DNA minor groove binding ability and one of them **5b** linked through the pentanedioxy chain exhibits efficient DNA binding ability ($\Delta T_m = 11.0^\circ\text{C}$) when compared to naturally occurring DC-81, **1** ($\Delta T_m = 0.7^\circ\text{C}$). The imine–amine PBD dimers exhibit promising in vitro antitumor activity in a number of human cancer cell lines.

© 2004 Elsevier Ltd. All rights reserved.

1. Introduction

Recently, the design and development of DNA interactive ligands that are capable of binding to DNA in a sequence selective manner^{1–3} has received considerable attention. In spite of rational design of synthetic DNA intercalators, there are few such compounds, which exhibit sequence selectivity that are in current clinical usage. These compounds with the ability to target and then down regulate individual genes have potential use as drugs for therapy of genetic based diseases including some cancers,⁴ and as research tools for using functional genomic studies.

The pyrrolo[2,1-*c*][1,4]benzodiazepines (PBDs) are a well known class of sequence selective DNA binding antitumor antibiotics derived from *Streptomyces* species.⁵ They exert their biological activity through covalent binding via their N10–C11 imine/carbinolamine

moiety to the C2-amino position of a guanine residue within the minor groove of DNA.⁶ Molecular modeling, solution NMR, fluorimetry, and DNA foot printing experiments have shown that these molecules have a preferred selectivity for Pu-G-Pu sequences^{7,8} and can be oriented with their A-rings pointed either toward the 3'- or 5' end of the covalently bonded DNA strand as in the case of naturally occurring anthramycin, tomaymycin, and DC-81 (**1**). The reduction of the imine functionality at N10–C11 of the DC-81 (**1**) provides the secondary amine form of DC-81 (**2**), which loses the covalent binding capability and could exhibit noncovalent interactions alone. The PBDs have been used to attach ethylenediaminetetraacetic acid (EDTA),⁹ epoxide,¹⁰ polyamide,¹¹ oligopyrrole,¹² and cyclopropylpyrroloindole (CPI)¹³ moieties leading to novel hybrids of PBD, which have exhibited sequence selective DNA-cleaving and cross-linking properties. Furthermore, there have been attempts to develop more potent compounds that could enhance the sequence selectivity as in case of C8 diether-linked PBD dimers DSB-120 (**3**),¹⁴ SJG-136,¹⁵ DRG-16,¹⁶ and C2–C3/C2'–C3' *endo* unsaturated PBD dimer.¹⁷ It has been observed that there has been extensive improvement in the biological activity due to the cross-linking property by the presence

Keywords: Pyrrolobenzodiazepines; DNA binding affinity; Cytotoxicity.

* Corresponding author. Tel.: +91 40 27193157; fax: +91 40 27193189; e-mail: ahmedkamal@iiict.res.in

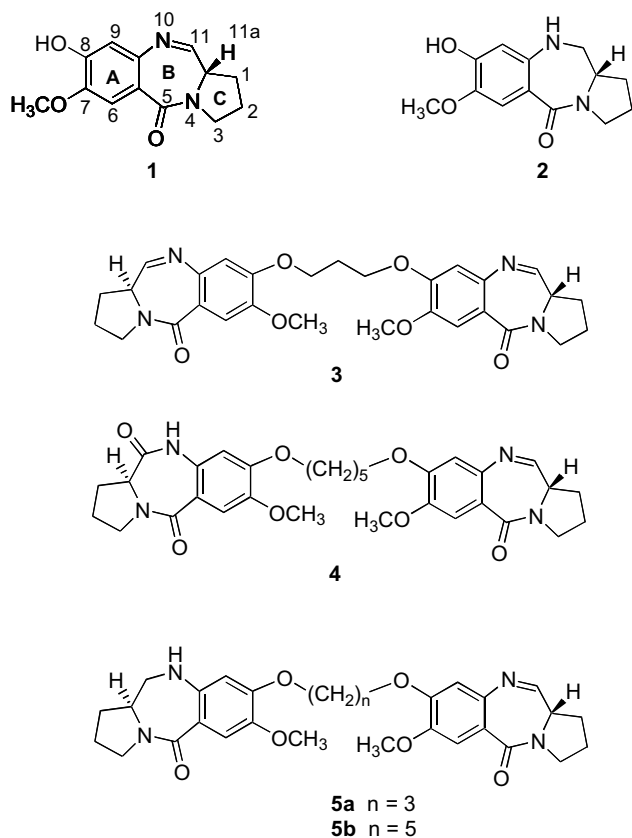


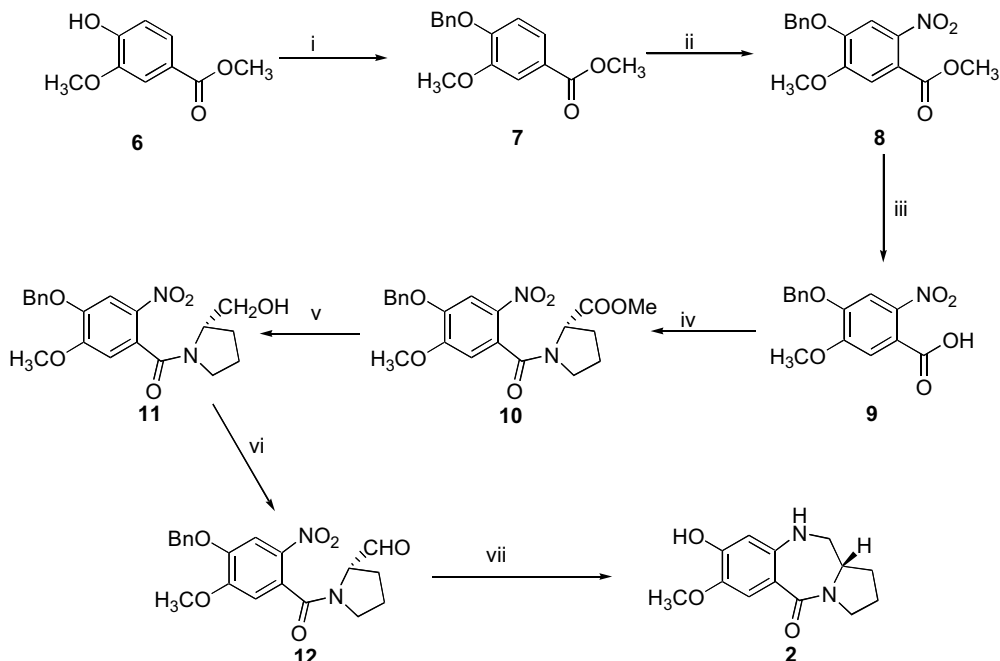
Figure 1. Structures of the PBD monomer DC-81 (**1**), PBD secondary amine (**2**), and PBD dimers, DSB-120 (**3**), mixed imine–amide PBD dimer (**4**) and **5**.

of two imine functionalities. We have been involved in the design and synthesis of PBD dimers with one imine functionality alone for exploring their DNA binding ability and cytotoxicity as noncross-linking agents and have also been interested in the design and synthesis of new PBD hybrids.^{18–27} In continuation of these efforts, it was considered significant to synthesize and evaluate mixed dimers of PBD that contain an imino functionality in one of the PBD rings and a secondary amine (N10) group in the other, which are linked at the C8 position by a suitable alkane spacer. Therefore, we herein report the synthesis and biological evaluation and molecular modeling studies of mixed imine–amine PBD dimers (Fig. 1).

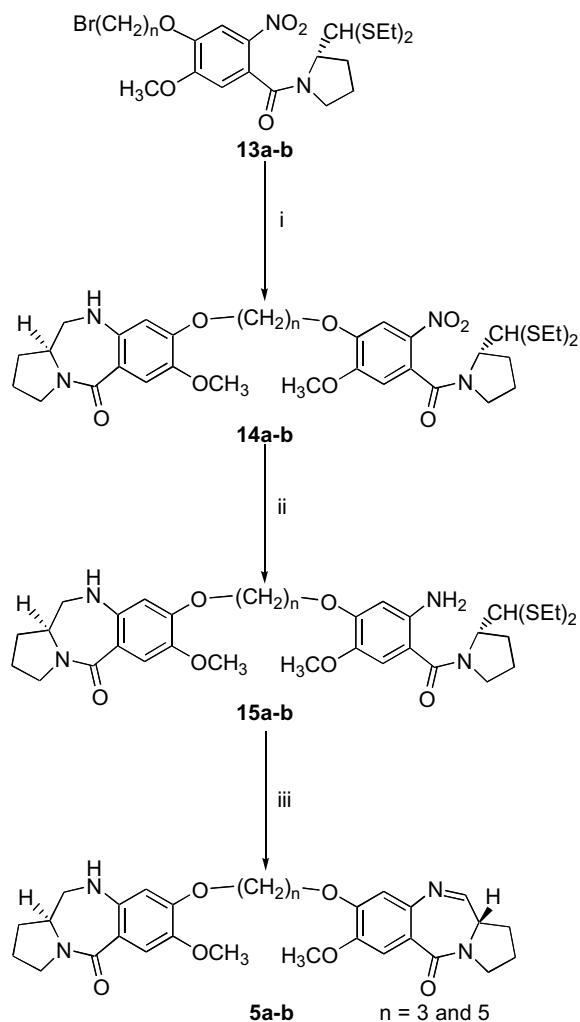
2. Results and discussion

2.1. Synthesis

Synthesis of the mixed imine–amine PBD dimers has been carried out employing methyl vanillate¹⁰ followed by benzylation, nitration, and ester hydrolysis to provide 4-benzyloxy-5-methoxy-2-nitrobenzoic acid **9**. L-Proline methyl ester hydrochloride has been coupled to compound **9** to afford compound **10**, which upon reduction followed by oxidation gives compound **12**. While compound **2** has been prepared from compound **12** by hydrogenation over Pd/C at 275.76×10^3 Pa (Scheme 1). The other precursors, (2*S*)-*N*-[*n*-(bromoalkoxy)-5-methoxy-2-nitrobenzoyl]pyrrolidine-2-carboxaldehyde diethyl thioacetals **13a–b** have been prepared by our previous method.¹⁹ The key intermediates **14a–b** have been prepared by linking **2** and **13a–b**,



Scheme 1. Reagents and conditions: (i) $C_6H_5CH_2Br$, K_2CO_3 , CH_3COCH_3 , reflux, 12 h, 92%; (ii) HNO_3 – $SnCl_4$, CH_2Cl_2 , –78%; (iii) 1 N LiOH, THF– H_2O –MeOH (3:1:1), room temperature, 12 h, 83%; (iv) $SOCl_2$, C_6H_6 , L-proline methylester hydrochloride, Et_3N , H_2O , THF, 0°C, 1 h, 85%; (v) $LiBH_4$, THF, 0°C, 2.5 h, 85%; (vi) $(COCl)_2$ /DMSO, TEA, CH_2Cl_2 , –70°C, 90%; (vii) Pd/C, H_2 , MeOH, room temperature, 8 h, 62%.



Scheme 2. Reagents and conditions: (i) compound **2**, K_2CO_3 , CH_3COCH_3 , reflux, 70–72%; (ii) $SnCl_2 \cdot 2H_2O$, MeOH, reflux, 78–80%; (iii) $HgCl_2$, $CaCO_3$, CH_3CN-H_2O (4:1), 50–51%.

there upon reduction gives **15a-b**. Finally, the deprotection of thioacetal functionality affords the desired mixed imine-amine PBD dimers **5a-b**, respectively (Scheme 2).

2.2. DNA interactions: thermal denaturation studies

The DNA binding affinity of the novel noncross-linking imine-amine PBD dimers (**5a-b**) has been investigated by thermal denaturation using calf thymus (CT)-DNA.²⁸ The studies for these compounds (**5a-b**) have been carried out at DNA/PBD molar ratios of 5:1. The increase in melting temperature (ΔT_m) for each compound is examined at 0 and 18h incubation at 37°C (Table 1). It is observed from the data that compound **5b** is an efficient stabilizing agent for double-stranded CT-DNA. This compound elevates the helix melting temperature of the CT-DNA by 11.0°C after incubation at 37°C for 18h. In the same experiment the naturally occurring DC-81 **1** gives a ΔT_m of 0.7°C and whereas synthetic DC-81 dimer **3** (DSB-120) gives a ΔT_m of 15.4°C. These results clearly demonstrate that compound **5b** containing a single imino functionality has a significant DNA binding affinity mainly due to

Table 1. Thermal denaturation data for DC-81 (**1**), DSB-120 (**3**), mixed imine-amine PBD dimer (**4**), and compounds **5a-b** with calf thymus DNA

PBD compound	[PBD]:[DNA] molar ratio ^b	Induced ΔT_m (°C) ^a after incubation at 37°C for	
		0h	18h
5a	1:5	8.7	9.7
5b	1:5	10.6	11.0
4	1:5	14.0	17.0
3	1:5	10.2	15.4
1	1:5	0.3	0.7

^a For CT-DNA alone at $pH 7.00 \pm 0.01$, $T_m = 69.2^\circ C \pm 0.01$ (mean value from 30 separate determinations), all ΔT_m values are ± 0.1 – $0.2^\circ C$.

^b For a 1:5 molar ratio of [ligand]/[DNA], where CT-DNA concentration = 100 μM and ligand concentration = 20 μM in aqueous sodium phosphate buffer [10mM sodium phosphate + 1 mM EDTA, $pH 7.00 \pm 0.01$].

noncovalent interactions. However, mixed imine-amine PBD dimer, **4** (five carbon chain linker) gives a ΔT_m of 17.0°C. It is interesting to note that the change of PBD dilactam (amide) subunit (**4**) to PBD secondary amine subunit in compound (**2**) slightly lowers the ΔT_m value. These results further exhibit that there is a decrease in the ΔT_m value for these mixed imine-amine PBD dimers (**5a**, **5b**) in comparison to the other noncross-linking mixed imine-amine PBD dimers (**4**) and this could be explained due to the absence of the carbonyl group in the noncovalent subunit part (**2**). Therefore, this investigation shows the importance of the carbonyl group for noncovalent interaction. As generally observed for the PBD dimers, compounds **5a-b** exert most of the effect upon the GC rich or high temperature regions of the DNA melting curves.

2.3. Cytotoxicity

Compounds **5a-b** have been evaluated in vitro against 60 human tumor cell lines derived from 9 cancer types (leukemia, nonsmall cell lung cancer, colon cancer, central nervous system cancer, melanoma, ovarian cancer, renal cancer, prostate cancer, and breast cancer). For each compound, dose response curves for each cell line have been measured at a minimum of five concentrations at 10-fold dilutions. A protocol of 48h continuous drug exposure is used, and a sulforhodamine B (SRB) protein assay has been used to estimate cell viability or growth. The concentration causing 50% cell growth inhibition (GI_{50}), total cell growth inhibition (TGI, 0% growth), and 50% cell death (LC_{50} , -50% growth) as compared with the control has been calculated. The mean graph midpoint (MG MID) values of log TGI and log LC_{50} as well as log GI_{50} for **5a-b** are listed in Table 2. As demonstrated by mean graph pattern (Fig. 2), compound **5a** exhibits an interesting profile of activity and selectivity for various cell lines. The MG MID of log TGI and log LC_{50} showed similar pattern to the log GI_{50} MG MID.

The GI_{50} values of compound **5a** (Table 3) against leukemia cancer CCRF-CEM, SR, and MOLT-4 cell

Table 2. Log GI_{50} , log TGI, and log LC_{50} MG MID of in vitro cytotoxicity data for compounds **5a–b** against human tumor cell lines^a

Compound	Log GI_{50}	Log TGI	Log LC_{50}
5a	-6.80	-5.73	-4.48
5b	-5.29	-4.55	-4.15

^a GI_{50} , drug molar concentration causing 50% cell growth inhibition; TGI, drug concentration causing total cell growth inhibition (0% growth); LC_{50} : drug concentration causing 50% cell death (-50%); MG MID, mean graph midpoints, the average sensitivity of all cell lines toward the test agent.

lines are <0.01, <0.01, and 0.01 μ M, respectively. In the nonsmall cell lung cancer panel, the growth of NCI-H 522 cell line is affected by compound **5a** with GI_{50} value as <0.01 μ M. Compound **5a** exhibits a cytotoxic potency in CNS cancer panel, in which SNB-75 and U251 cell lines are affected, with GI_{50} values of 0.02 μ M. Compound **5b** (Table 3) exhibited cytotoxic potency against leukemia cancer cell lines CCRF-CEM and SF, with GI_{50} values of 0.2 and 0.3 μ M, respectively, and it also exhibited cytotoxicity against renal cancer SN12C cell line, with GI_{50} value of 0.5 μ M.

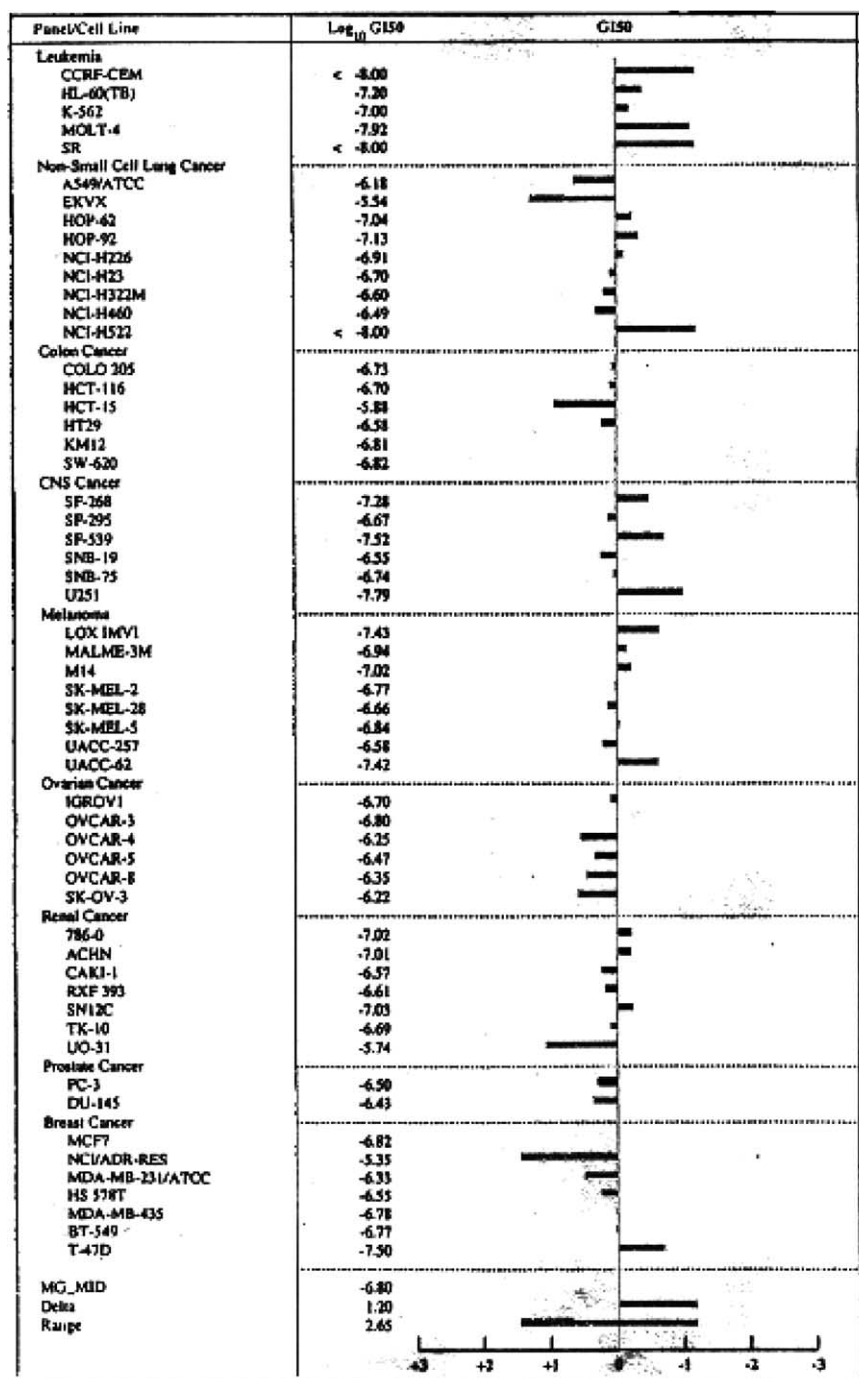
**Figure 2.** Log₁₀ GI_{50} data from the NCI 60 cell line screen for PBD compound **5a**.

Table 3. In vitro cytotoxicity of compound **5a** and **5b** in selected human cancer cell lines

Cancer panel/cell line	GI ₅₀ (μM)	
	5a	5b
<i>Leukemia</i>		
CCRF-CEM	<0.01	0.2
SR	<0.01	0.3
MOLT-4	0.01	—
<i>Nonsmall cell lung</i>		
NCI-H22	<0.01	—
<i>Central nervous system</i>		
SNB-75	0.02	—
U251	0.02	—
<i>Renal</i>		
SN12C	0.9	0.5

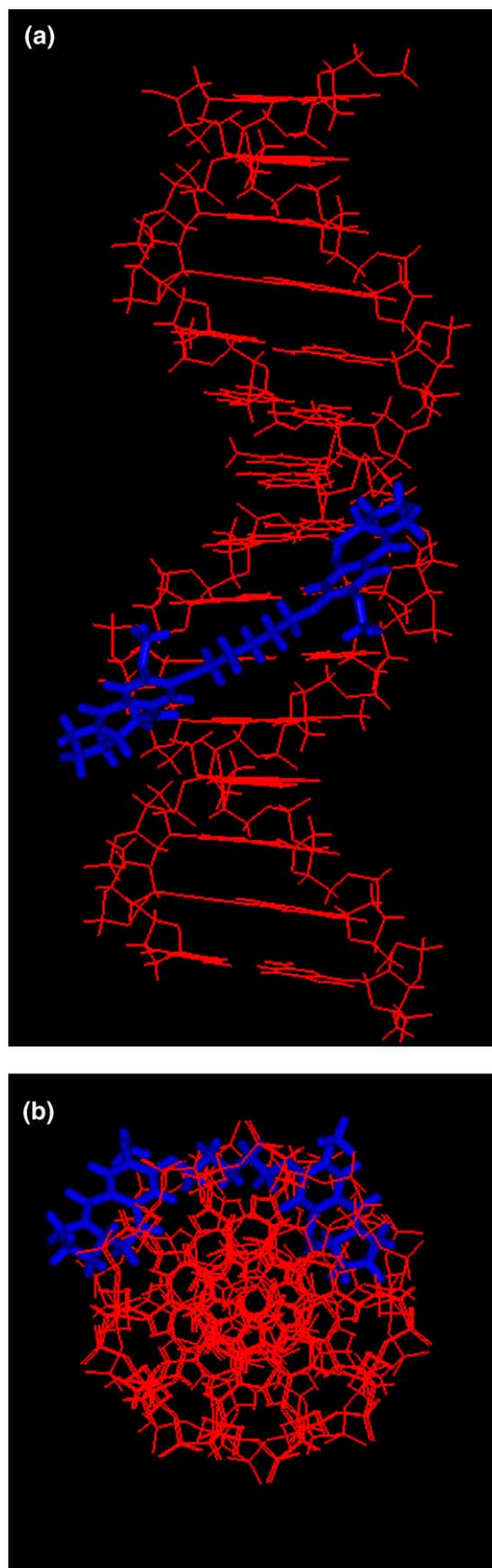
The comparison of the data in Table 3 reveals the importance of alkane spacer. Surprisingly, as the alkane spacer increases from three to five the cytotoxic activity moderately decreases and therefore, the DNA binding ability of these compounds could not be correlated to the cytotoxicity.

2.4. Molecular modeling studies

Modeling of the complexes of PBD dimers **1**, **4**, **5a**, and **5b** with the B-DNA duplex structure has been carried out as described in the methods section. A B-DNA duplex structure has been considered with a sequence 5'-GGGGAGAGAGAGGGG-3'—a symmetric sequence about the central triplet AGA, which is the most preferred site for PBD binding.⁵ Each of the DNA–PBD complexes has been subjected to molecular dynamics (MD) simulations followed by energy minimization of 'snap shots' collected at regular time intervals during the MD simulations. After energy minimization all the energy minima obtained have been compared with each other and the one with the lowest energy has been picked as the representative of the DNA–PBD complex (Fig. 3). The least energy complex thus picked up has been selected to calculate the interaction energy as a measure of stability of complex.

The interaction energies between DNA and PBDs are given in Table 4. It can be seen from this table that the imine–amide PBD dimer **4** renders more stability to the complex compared to the imine–amine PBD dimers (**5a** and **5b**), and the PBD monomer **1**. This property correlates with the experimentally determined values of the DNA melting temperature in these complexes (Fig. 4).

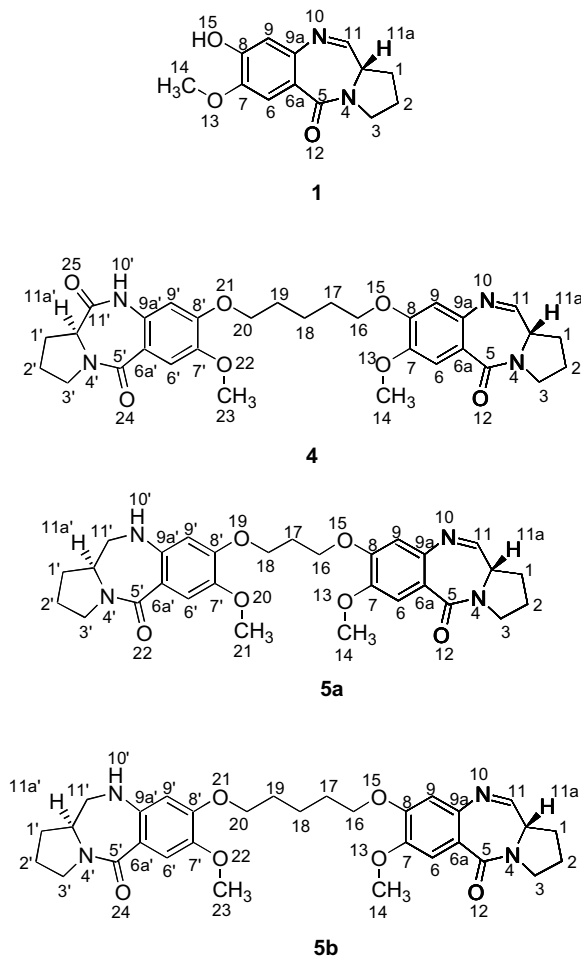
The complexes are characterized by the presence of a number of nonbonded interactions (Table 4) formed between DNA and PBD molecules in addition to the covalent linkage formed between the imine PBD subunit and exocyclic C2-amino group of the guanine (G8). The dimeric PBDs (**4**, **5a**, and **5b**) offer more favorable nonbonded interactions as compared to the monomeric

**Figure 3.** Projection diagram showing the DNA-**5b** complex; (a) side-on view; (b) down the helix axis.

DC-81 (**1**) and this is evident from their respective nonbonded energy terms (Table 4), which are about

Table 4. The values of energy of interactions calculated for the DNA–PBD dimer complexes

PBD compound	Total interaction energy (kcal mol ⁻¹)	Bonded interaction energy (kcal mol ⁻¹)	Nonbonded interaction energy (kcal mol ⁻¹)	
			van der Waals interaction energy (kcal mol ⁻¹)	Coulombic interaction energy (kcal mol ⁻¹)
1	-85.2	-14.2	-33.7	-37.3
4	-145.9	-12.2	-84.3	-49.4
5a	-132.1	-12.6	-71.8	-47.7
5b	-143.6	-14.8	-68.7	-60.1

**Figure 4.** Numbering of PBD ring systems.

50 kcal mol⁻¹ less as compared to DC-81. Among the dimeric PBDs the imine–amide PBD dimer **4** is associated with the lowest nonbonded energy term and is stabilized by the hydrogen bonding interaction between the carbonyl functionality and the amino group of **G12**. This hydrogen bonding is precluded in **5a** and **5b** because of the absence of the required carbonyl functionality (see Table 5). Between **5a** and **5b**, the latter is associated with better nonbonded as well as bonded energy components and these together render higher stability for **5b** by about 11 kcal mol⁻¹ as compared to **5a**.

The modeling of the complex of DNA with the cross-linking PBD dimer **3** has not been considered in the present study. In this the stability of the complex is predominantly due to the presence of additional covalent

interaction whereas in the noncross-linking molecules nonbonded interactions play an important role in stabilization of their respective complexes.

3. Conclusions

The DNA binding ability for these noncross-linking PBD dimers is noticeable in spite of the introduction of amine functionality in one of the PBD rings in comparison to DC-81. Modeling studies suggest that apart from the covalent linkage formed between the imine PBD subunit and G8, there are a number of favorable van der Waals and coulombic interactions that are formed between the DNA and the mixed imine–amine PBD dimer. The complex formed by compound **5b** (with a five carbon chain linker) is energetically more stable than the complex formed by **5a** as the extra alkane spacer units offer the molecule to make extra favorable van der Waals and coulombic interactions with DNA. However, **5b** exhibits lower ΔT_m value in comparison to **4** because of the absence of carbonyl functionality in the complex. Of all the molecules imine–amide PBD dimer **4** forms the most stable complex. Nevertheless, the imine–amine PBD dimers also exhibit interesting profile of DNA binding ability in contrast to PBD monomer (DC-81). This investigation exhibits the role played by noncovalent interaction of PBD secondary amine subunit. In addition these compounds show promising in vitro cytotoxicity in different cancer cell lines.

4. Experimental section

4.1. Synthetic chemistry

Reaction progress was monitored by thin-layer chromatography (TLC) using GF₂₅₄ silica gel with fluorescent indicator on glass plates. Visualization was achieved with UV light and iodine vapor unless otherwise stated. Chromatography was performed using Acme silica gel (100–200 mesh). The majority of reaction solvents were purified by distillation under nitrogen from the indicated drying agent and used fresh: dichloromethane (calcium hydride), tetrahydrofuran (sodium benzophenone ketyl), methanol (magnesium methoxide), acetonitrile (calcium hydride).

¹H NMR spectra were recorded on Varian Gemini 200/300 MHz spectrometer using tetramethyl silane (TMS) as an internal standard. Chemical shifts are reported in parts per million (ppm) down field from tetramethyl-

Table 5. List of hydrophobic contacts and hydrogen bonded interactions (Fig. 4)

	DC-81	4	5a	5b
<i>Hydrophobic interactions</i>				
	G8.C2'...C1	G8.C2'...C1	G8.C2'...C1	G8.C2'...C1
	A9.C2'...C1	A9.C2'...C1	A9.C2'...C1	A9.C2'...C1
	G10.C2'...C6	G10.C2'...C6	G10.C2'...C9	G10.C2'...C9
	C8.C2'...C9	A11.C2'...C19	A11.C2'...C9'	A11.C2'...C18
	T9.C2'...C6a	G12.C2'...C9'	G12.C2'...C6'a	G12.C2'...C9'
	C10.C2'...C2	G13.C2'...C1'	G13.C2'...C1'	G13.C2'...C1'
		C6.C2'...C6'a	C6.C2'...C1'	C6.C2'...C1'
		T7.C2'...C9'	T7.C2'...C6'a	T7.C2'...C9'
		C8.C2'...C9	C8.C2'...C9	C8.C2'...C9
		T9.C2'...C9	T9.C2'...C6a	T9.C2'...C6a
		C10.C2'...C2	C10.C2'...C2	C10.C2'...C2
<i>Hydrogen bonded interactions^a</i>				
	C8.O2...N10	G12.N2...O25	C8.O2...N10	C8.O2...N10
	C8.O2...N10			

^a Imine N of PBD in all the complexes (**1**, **4**, **5a**, and **5b**) is at a favorable distance (~3.3) to imino group of A9 of DNA however the angle is not within hydrogen bonding limits (N–H...N ~ 77°).

silane. Spin multiplicities are described as s (singlet), brs (broad singlet), d (doublet), t (triplet), q (quartet), m (multiplet). Coupling constants are reported in Hertz (Hz). Low resolution mass spectra were recorded on VG-7070H Micromass mass spectrometer at 200 °C, 70eV with trap current of 200 μA and 4kV acceleration voltage. HRMS were recorded on VG Autospec N mass spectrometer at 200 °C, 70eV with a trap current of 200 μA and 7kV acceleration voltage.

4.1.1. Methyl 4-benzyloxy-3-methoxybenzoate (7). To a solution of vanillin methyl ester **6** (182mg, 1mmol) in acetone (30mL) was added, anhydrous K₂CO₃ (553mg, 4mmol) and benzyl bromide (256mg, 1.5mmol), the mixture was refluxed in an oil bath for 24h. The reaction was monitored by TLC using EtOAc–hexane (2:8) and K₂CO₃ was removed by filtration and the solvent was evaporated under the vacuum and was purified by column chromatography (10% EtOAc–hexane) to afford compound **7** as white solid (250mg, 92%); mp 117–118 °C. ¹H NMR (CDCl₃) δ 3.94 (s, 3H), 3.98 (s, 3H), 5.20 (s, 2H), 6.88 (d, 1H, *J* = 8.2Hz), 7.20–7.50 (m, 5H), 7.50–7.60 (m, 2H); MS (EI) *m/z* 272 [M]⁺.

4.1.2. Methyl 4-benzyloxy-5-methoxy-2-nitrobenzoate (8). A freshly prepared mixture of stannic chloride (301mg, 1.156mmol) and fuming nitric acid (98mg, 1.56mmol) in dichloromethane was added dropwise over 5min with stirring to a solution of methyl-4-benzyloxy-3-methoxybenzoate **7** (272mg, 1mmol) in dichloromethane (30mL) at –78 °C (dry ice/acetone). The mixture was maintained at –78 °C for a further 5min, quenched with water (20mL), and then allowed to return to room temperature. The organic layer was separated and the aqueous layer was extracted with dichloromethane (2 × 20mL). The combined organic phase dried (Na₂SO₄), evaporated in vacuum, and it was purified by column chromatography (20% EtOAc–hexane) to give **8** as a yellow solid (247mg, 78%); mp 128–132 °C. ¹H NMR (CDCl₃) δ 3.89 (s, 3H), 3.95 (s,

3H), 5.20 (s, 2H), 7.05 (s, 1H), 7.20–7.45 (m, 5H), 7.50 (s, 1H); MS (EI) *m/z* 317 [M]⁺.

4.1.3. 4-Benzyloxy-5-methoxy-2-nitrobenzoic acid (9). Lithium hydroxide monohydrate (2N, 1.22mL) was added to a solution of methyl 4-benzyloxy-5-methoxy-2-nitrobenzoate **8** (317mg, 1mmol) in THF–H₂O–MeOH (4:1:1) and the mixture was stirred at room temperature for 12h. After most of the THF and methanol were evaporated, the aqueous phase was acidified with 12N HCl to pH 7 and re-extracted with CH₂Cl₂ to give a 4-benzyloxy-5-methoxy-2-nitrobenzoic acid **9** as a pale yellow solid (251mg, 83%); mp 180–183 °C. ¹H NMR (CDCl₃) δ 3.98 (s, 3H), 5.20 (s, 2H), 7.20 (s, 1H), 7.35–7.55 (m, 6H); MS (EI) *m/z* 303 [M]⁺.

4.1.4. Methyl (2S)-N-[4-benzyloxy-5-methoxy-2-nitrobenzoyl]pyrrolidine-2-carboxylate (10). To a stirred suspension of compound **9** (303mg, 1mmol) and thionyl chloride (476mg, 4.0mmol) in dry benzene (15mL) was added DMF (four to five drops) and the stirring was continued for 6h. The benzene was evaporated in vacuum and the resultant oil dissolved in dry THF (20mL) and added dropwise over a period of 30min to a stirred suspension of L-proline methyl ester hydrochloride (247mg 1.5mmol), triethylamine (303mg, 3mmol), and ice water (20mL) cooled in an ice bath. After the completion of addition, the reaction mixture was brought to ambient temperature and stirred for an additional hour. The THF was evaporated in vacuum and the aqueous layer was washed with ethyl acetate (10mL). The aqueous phase was then adjusted to pH 3 using 6N HCl and extracted with ethyl acetate and washed with brine, dried over Na₂SO₄, evaporated in vacuum, and was purified by column chromatography (30% EtOAc–hexane) to afford compound **10** as yellow oil (352mg, 85%). ¹H NMR (CDCl₃) δ 1.85–2.12 (m, 3H), 2.20–2.45 (m, 1H), 3.10–3.25 (m, 1H), 3.26–3.40 (m, 1H), 3.80 (s, 3H), 3.92 (s, 3H), 4.68–4.75 (m, 1H), 5.20 (s, 2H), 6.82 (s, 1H), 7.30–7.48 (m, 5H), 7.72 (s, 1H); MS (EI) *m/z* 414 [M]⁺.

4.1.5. (2S)-N-[4-Benzyloxy-5-methoxy-2-nitrobenzoyl]-2-(hydroxymethyl)pyrrolidine (11). A solution of ester **10** (414 mg, 1 mmol) in THF (20 mL) was cooled to 0 °C and treated portion-wise with LiBH₄ (33 mg, 1.5 mmol). The stirred reaction mixture was allowed to warm to room temperature over 2.5 h under an N₂ atmosphere, after which TLC revealed the complete consumption of starting material. The mixture was cooled to 0 °C and carefully treated with water (18 mL) and then 2 N HCl (5 mL). After concentration in vacuum, the mixture was adjusted to pH 7 with 10 N NaOH saturated with solid NaCl and then extracted with EtOAc (50 mL). The combined organic phase was washed with brine (20 mL), dried (Na₂SO₄), filtered, and evaporated in vacuum to furnish the pure alcohol **11** as oil (328 mg, 85%). ¹H NMR (CDCl₃) δ 1.65–2.20 (m, 4H), 2.80–3.20 (brs, OH, exchangeable) 3.18–3.28 (m, 2H), 3.65–3.90 (m, 2H), 4.0 (s, 3H), 4.20–4.40 (m, 1H), 5.20 (s, 2H), 7.0 (s, 1H), 7.28–7.50 (m, 5H), 7.75 (s, 1H); MS (EI) *m/z* 355 [M – CH₂OH]⁺.

4.1.6. (2S)-N-[4-Benzyloxy-5-methoxy-2-nitrobenzoyl]-pyrrolidine-2-carbaldehyde (12). A solution of DMSO (0.60 mL, 8.4 mmol) in CH₂Cl₂ (10 mL) was added dropwise to a cooled solution of oxalyl chloride (0.46 mL, 5.33 mmol) at –60 °C (dry ice/acetone) under an N₂ atmosphere. After the mixture was stirred at –70 °C for 45 min and then the alcohol **11** (1.15 g, 3 mmol) dissolved in 25 mL of dry CH₂Cl₂ was added dropwise at –60 °C. The reaction mixture was allowed to stir for 1.5 h at –70 °C. Then a solution of TEA (1.67 mL, 12 mmol) in 15 mL of dry CH₂Cl₂ was added dropwise and the mixture was allowed to warm room temperature. The reaction mixture was diluted with water (50 mL), extracted with 1 N HCl (25 mL), saturated aqueous NaHCO₃ (25 mL), and then brine (25 mL). The organic solution was dried over Na₂SO₄ and evaporated under vacuum. The residue was purified by column chromatography (30% EtOAc–hexane) to afford compound **12** as yellow oil (345 mg, 90%). ¹H NMR (CDCl₃) δ 1.88–2.40 (m, 5H), 3.18–3.38 (m, 2H), 4.02 (s, 3H), 4.70 (m, 1H), 5.22 (s, 2H), 6.86 (s, 1H), 7.25–7.50 (m, 5H), 7.75 (s, 1H), 9.25 (s, 1H), 9.80 (s, 1H); MS (EI) *m/z* 355 [M – CHO]⁺.

4.1.7. (11aS)-8-Hydroxy-7-methoxy-1,2,3,10,11,11a-hexahydro-5H-pyrrolo[2,1-c][1,4]benzodiazepine-5-one (2). The compound **12** (384 mg, 1.0 mmol) was dissolved in methanol (10 mL) and 10% Pd–C (200 mg) was added. The mixture was hydrogenated at room temperature under atmospheric pressure for 10 h. The catalyst was removed by filtration through Celite, then the solvent was evaporated under vacuum and purified by column chromatography (80% EtOAc–hexane) to afford **2** as fluffy solid (154 mg, 62%); mp 278–280 °C. ¹H NMR (CDCl₃) δ 1.70–2.35 (m, 4H), 3.19–3.29 (m, 1H), 3.45–3.55 (m, 1H), 3.55–3.75 (m, 2H), 3.75–3.85 (m, 1H), 3.85 (s, 3H), 6.08 (s, 1H), 7.50 (s, 1H); MS (EI) *m/z* 248 [M]⁺.

4.1.8. (2S)-N-[4-[3-(7-Methoxy-(11aS)-1,2,3,10,11,11a-hexahydro-5H-pyrrolo[2,1-c][1,4]benzodiazepine-5-one-8-yloxy)propoxy]-5-methoxy-2-nitrobenzoyl]pyrrolidine-2-carbaldehyde diethyl thioacetal (14a). To a solution of

(2S)-N-[4-(3-bromo-propoxy)-5-methoxy-2-nitrobenzoyl]pyrrolidine-2-carbaldehyde diethyl thioacetal **13a** (521 mg, 1 mmol) in dry acetone (30 mL) was added anhydrous K₂CO₃ (553 mg, 4 mmol) and the (11aS)-8-hydroxy-7-methoxy-1,2,3,10,11,11a-hexahydro-5H-pyrrolo-[2,1-c][1,4]benzodiazepine-5-one **2** (248 mg, 1 mmol). The reaction mixture was refluxed in an oil bath for 48 h. The reaction was monitored by TLC using EtOAc–hexane (9:1) as a solvent system. K₂CO₃ was removed by filtration and the solvent was removed under vacuum. The crude product was purified by column chromatography (90% EtOAc–hexane) to afford a yellow oil **14a** (482 mg, 70%). ¹H NMR (CDCl₃) δ 1.35–1.45 (m, 6H), 1.70–2.45 (m, 10H), 2.72–2.90 (m, 4H), 3.20–3.28 (m, 4H), 3.50–3.58 (m, 1H), 3.62–3.75 (m, 1H), 3.80–3.90 (m, 4H), 3.92–3.98 (m, 3H), 4.20 (t, 2H, *J* = 6.0 Hz), 4.35 (t, 2H, *J* = 6.1 Hz), 4.65–4.75 (m, 1H), 4.85 (d, 1H, *J* = 4.28 Hz), 6.08 (s, 1H), 6.80 (s, 1H), 7.58 (s, 1H), 7.72 (s, 1H); MS (FAB) 689 [M + H]⁺.

4.1.9. (2S)-N-[4-[5-(7-Methoxy-(11aS)-1,2,3,10,11,11a-hexahydro-5H-pyrrolo[2,1-c][1,4]benzodiazepine-5-one-8-yloxy)pentyl]-5-methoxy-2-nitrobenzoyl]pyrrolidine-2-carbaldehyde diethyl thioacetal (14b). The compound **14b** was prepared according to the method described for **14a** by employing the (11aS)-8-hydroxy-7-methoxy-1,2,3,10,11,11a-hexahydro-5H-pyrrolo[2,1-c][1,4]benzodiazepine-5-one **2** and **13b** (549 mg, 1 mmol) to afford **14b** as yellow oil (516 mg, 72%). ¹H NMR (CDCl₃) δ 1.30–1.40 (m, 6H), 1.65–2.35 (m, 14H), 2.65–2.75 (m, 4H), 3.18–3.32 (m, 3H), 3.45–3.75 (m, 2H), 3.80–3.85 (m, 4H), 3.85–4.0 (m, 5H), 4.65–4.72 (m, 1H), 4.85 (d, 1H, *J* = 4.38 Hz), 6.0 (s, 1H), 6.78 (s, 1H), 7.52 (s, 1H), 7.65 (s, 1H); MS (FAB) 717 [M + H]⁺.

4.1.10. (2S)-N-[4-[3-(7-Methoxy-(11aS)-1,2,3,10,11,11a-hexahydro-5H-pyrrolo[2,1-c][1,4]benzodiazepine-5-one-8-yloxy)propoxy]-5-methoxy-2-aminobenzoyl]pyrrolidine-2-carbaldehyde diethyl thioacetal (15a). The compounds **14a** (688 mg 1 mmol) dissolved in methanol (20 mL) and added SnCl₂·2H₂O (1.125 g, 5 mmol) was refluxed for 1.5 h or until the TLC indicated that reaction was complete. The methanol was evaporated by vacuum and the aqueous layer was then carefully adjusted to pH 8 with 10% NaHCO₃ solution and then extracted with ethyl acetate (2 × 30 mL). The combined organic phase was dried over Na₂SO₄ and evaporated under vacuum to afford the amino diethyl thioacetal **15a** as a yellow oil, which due to potential stability problems,²⁹ was briefly characterized by ¹H NMR and then used directly in the next step (514 mg, 78%). ¹H NMR (CDCl₃) δ 1.20–1.42 (m, 6H), 1.60–2.42 (m, 10H), 2.60–2.85 (m, 4H), 3.18–3.28 (m, 2H), 3.40–3.75 (m, 5H), 3.78 (s, 3H), 3.85 (s, 3H), 4.05–4.25 (m, 4H), 4.60–4.70 (m, 2H), 6.05 (s, 1H), 6.25 (s, 1H), 6.80 (s, 1H), 7.52 (s, 1H).

4.1.11. (2S)-N-[4-[5-(7-Methoxy-(11aS)-1,2,3,10,11,11a-hexahydro-5H-pyrrolo[2,1-c][1,4]benzodiazepine-5-one-8-yloxy)pentyl]-5-methoxy-2-aminobenzoyl]pyrrolidine-2-carbaldehyde diethyl thioacetal (15b). The compound **15b** was prepared according to the method described for the compound **15a** employing the compound **14a** (716 mg, 1 mmol) to afford the amino diethyl thioacetal

15b as a yellow liquid (550 mg, 80%). ^1H NMR (CDCl_3) δ 1.20–1.40 (m, 6H), 1.50–2.38 (m, 14H), 2.60–2.80 (m, 4H), 3.10–3.25 (m, 2H), 3.40–3.68 (m, 5H), 3.68–4.0 (m, 10H), 4.58–4.65 (m, 2H), 4.65–5.10 (brs, 2H), 6.0 (s, 1H), 6.20 (s, 1H), 6.78 (s, 1H), 7.48 (s, 1H).

4.1.12. 7-Methoxy-8-{3-[7-methoxy-(11a*S*)-1,2,3,10,11,11a-hexahydro-5*H*-pyrrolo[2,1-*c*]-[1,4]benzodiazepine-5-one-8-yloxy]propoxy}-(11a*S*)-1,2,3,11a-tetrahydro-5*H*-pyrrolo[2,1-*c*][1,4]benzodiazepin-5-one (5a**).** A solution of **15a** (658 mg, 1 mmol), HgCl_2 (613.6 mg, 2.26 mmol) and CaCO_3 (246 mg, 2.46 mmol) in MeCN–water (4:1) was stirred slowly at room temperature until TLC indicates complete loss of starting material (12 h). The reaction mixture was diluted with EtOAc (30 mL) and filtered through a Celite bed. The clear yellow organic supernatant was extracted with saturated 5% NaHCO_3 (20 mL), brine (20 mL) and the combined organic phase is dried (Na_2SO_4). The organic layer was evaporated in vacuum and purified by column chromatography (90% MeOH–EtOAc) to give compound **5a** as pale yellow oil (267 mg, 50%). This material was repeatedly evaporated from CHCl_3 in vacuum to generate the imine form. ^1H NMR (CDCl_3) δ 1.65–2.45 (m, 10H), 3.15–3.25 (m, 2H), 3.48–3.75 (m, 4H), 3.78–3.88 (m, 4H), 3.90 (s, 3H), 4.25–4.35 (m, 5H), 6.18 (s, 1H), 6.82 (s, 1H), 7.48 (s, 1H), 7.52 (s, 1H), 7.65 (d, 1H, $J = 4.8$ Hz); MS (FAB) 535 $[\text{M} + \text{H}]^+$; HRMS $[\text{M} + \text{H}]^+$ calcd for $\text{C}_{29}\text{H}_{35}\text{N}_4\text{O}_6$ m/z 535.255660, obsd (FAB) m/z 535.257085; $[\alpha]_{\text{D}}^{25} + 530.3$ (c 0.5, CHCl_3); reverse phase HPLC (C_8 stationary phase, 85% MeOH/ H_2O mobile phase, 254 nm) $t_{\text{R}} = 4.21$ min, % peak area = 99.0%; calcd for $\text{C}_{29}\text{H}_{34}\text{N}_4\text{O}_6$: C, 65.15; H, 6.41; N, 10.48; found: C, 65.40; H, 6.31; N, 10.22.

4.1.13. 7-Methoxy-8-{5-[7-methoxy-(11a*S*)-1,2,3,10,11,11a-hexahydro-5*H*-pyrrolo[2,1-*c*]-[1,4]benzodiazepine-5-one-8-yloxy]pentyl}-(11a*S*)-1,2,3,11a-tetrahydro-5*H*-pyrrolo[2,1-*c*][1,4]benzodiazepin-5-one (5b**).** The compound **5b** was prepared according to the method described for the compound **5a** employing **15b** (686 mg, 1 mmol) to afford **5b** as a pale yellow oil (287 mg, 51%). ^1H NMR (CDCl_3) δ 1.20–2.45 (m, 14H), 3.10–3.20 (m, 2H), 3.20–3.28 (m, 1H), 3.40–3.78 (m, 5H), 3.80 (s, 3H), 3.98 (s, 3H), 4.10–4.22 (m, 4H), 6.0 (s, 1H), 7.02 (s, 1H), 7.50 (s, 1H), 7.55 (s, 1H), 7.65 (d, 1H, $J = 4.4$ Hz); ^{13}C NMR (CDCl_3) δ 22.4, 22.8, 24.1, 28.6, 29.5, 30.8, 46.6, 48.3, 52.9, 53.6, 56.1, 57.7, 68.4, 68.7, 102, 110.5, 111.6, 115.3, 120.1, 140.6, 141.2, 142.1, 147.8, 150.8, 152, 163.3, 164.6, 166.3; MS (FAB) 563 $[\text{M} + \text{H}]^+$; HRMS $[\text{M} + \text{H}]^+$ calcd for $\text{C}_{31}\text{H}_{39}\text{N}_4\text{O}_6$ m/z 563.286960, obsd (FAB) m/z 563.288484; $[\alpha]_{\text{D}}^{25} + 472.6$ (c 0.5, CHCl_3); reverse phase HPLC (C_8 stationary phase, 85% MeOH/ H_2O mobile phase, 254 nm) $t_{\text{R}} = 4.22$ min, % peak area = 97.3%; calcd for $\text{C}_{31}\text{H}_{38}\text{N}_4\text{O}_6$: C, 66.17; H, 6.81; N, 9.96; found: C, 66.39; H, 6.56; N, 9.65.

4.2. Thermal denaturation studies

Compounds were subjected to thermal denaturation studies with duplex-form CT-DNA using by reported

method.²⁸ Working solutions in aqueous buffer (10 mM $\text{NaH}_2\text{PO}_4/\text{Na}_2\text{HPO}_4$, 1 mM Na_2EDTA , pH 7.00 + 0.01) containing CT-DNA (100 μm in phosphate) and the PBD (20 μm) were prepared by addition of concentrated PBD solutions in MeOH to obtain a fixed $[\text{PBD}]/[\text{DNA}]$ molar ratio of 1:5. The DNA–PBD solutions were incubated at 37 °C for 0, 18 h prior to analysis. Samples were monitored at 260 nm using a Beckman DU-7400 spectrophotometer fitted with high performance temperature controller, and heating was applied at 1 °C min^{-1} in the 40–90 °C range. DNA helix \rightarrow coil transition temperatures (T_{m}) were obtained from the maxima in the $d(A_{260})/dT$ derivative plots. Results are given as the mean \pm standard deviation from three determinations and are corrected for the effects of MeOH co-solvent using a linear correction term.³⁰ Drug-induced alterations in DNA melting behavior are given by: $\Delta T_{\text{m}} = T_{\text{m}}(\text{DNA} + \text{PBD}) - T_{\text{m}}(\text{DNA alone})$, where the T_{m} value for the PBD-free CT-DNA is 69.2 \pm 0.01 °C. The fixed $[\text{PBD}]/[\text{DNA}]$ ratio used did not result in binding saturation of the host DNA duplex for any compound examined.

4.3. Molecular modeling studies

Calculations were performed using INSIGHT-II suite of software (MSI, Inc.) running on Silicon Graphics OCTANE system. The strategy and protocol used for molecular modeling is similar to that adopted in our previous study.¹⁹

(a) *Modeling of DNA duplex and PBD dimer structures.* The 15-mer DNA sequence GGGGAGAGAGAGGGG a symmetric sequence about the central triplet AGA, which is the most preferred site for PBD binding was considered. BIOPOLYMER module was used to build the B-DNA duplex structure. PBD dimers **1**, **4**, **5a**, and **5b** were separately constructed using the BUILDER module of INSIGHT-II. Initially PBDs were ‘sketched’ in 2D (two dimensions) and then converted into 3D (three dimensions) using 2d–3d converter tool of the BUILDER module. Care was taken to see that there is C11(*S*)-geometry for all PBD dimers constructed, as this stereochemistry is known to lead to energetically favored adduct with that of guanine of B-DNA duplex structure.⁵

(b) *Docking studies.* PBDs were manually docked into the minor groove of B-DNA duplex such that the N10–C11 imine functionality and the exocyclic C2-amino group of guanine (G8) are nearly at bonding distance and a covalent bond was then formed using the create-bond tool. After the bond was created, the PBDs in the minor groove were manually oriented such that the PBDs are oriented toward the 3' end of covalently linked B-DNA duplex strand. Dihedral angles about C–C bonds were manually adjusted so that PBD dimers form an isohelical fit within the minor groove of the B-DNA duplex structure. CVFF force field was used to fix the charges and the potentials required for energy calculations. The complexes formed were subjected to energy minimization (EM) using conjugate gradient method till they were fully converged that is, till the energy gradient

was nearly equal to 0.001 kJ mol⁻¹ nm. Constraints were applied to fix the B-DNA duplex structure during EM.

(c) *Molecular dynamics.* Molecular dynamic studies were carried using the following protocol: heating phase (equilibration) = 30 ps and sampling phase = 100 ps. During simulations constraints were applied to fix the B-DNA duplex structure. Intermittent structures of the complex formed at every 10 ps of simulation were collected and subjected to EM. The minima of all the snap shots were examined in order to select the lowest energy conformation as a representative of DNA–PBD complex for further studies.

(d) *Energy of interaction.* The energy of the PBD–DNA complex (E_{complex}) and the energies of DNA (E_{DNA}) and PBD (E_{PBD}) individually after separating from the complex were calculated. Energy of interaction (E_{int}) between DNA and PBD complex were calculated using the following formula:

$$E_{\text{int}} = E_{\text{complex}} - (E_{\text{DNA}} + E_{\text{PBD}})$$

where E_{int} = energy of interaction of the complex, E_{complex} = total energy of the complex, E_{DNA} and E_{PBD} are the individual total energies of the DNA and the PBD molecules calculated after they are separated from each other.

Acknowledgements

We thank the National Cancer Institute, Maryland for in vitro anticancer assay in human cancer cell lines. The authors G.R., O.S., P.R., and N.L. are thankful to CSIR, New Delhi for the award of research fellowships.

References and notes

- Cooper, N.; Hagan, D. R.; Tiberghien, A.; Ademefun, T.; Matthews, C. S.; Howard, P. W.; Thurston, D. E. *Chem. Commun.* **2002**, 1764.
- White, S.; Szewczyk, J. W.; Turner, J. M.; Baird, E. E.; Dervan, P. B. *Nature* **1998**, *391*, 468.
- Thurston, D. E. *Br. J. Cancer* **1999**, *80*, 65.
- Neidle, S.; Thurston, D. E. In *New Targets for Cancer Chemotherapy*; Kerr, D. J., Workmann, P., Eds.; CRC: London, 1994; p 159.
- Thurston, D. E. *Molecular Aspects of Anticancer Drug–DNA Interactions*; Macmillan: London, 1993; p 54.
- Petrusek, R. L.; Uhlenhopp, E. L.; Duteau, N.; Hurley, L. H. *J. Biol. Chem.* **1982**, *257*, 6207.
- Hurley, L. H.; Reck, T.; Thurston, D. E.; Langley, D. R.; Holden, K. G.; Hertzberg, R. P.; Hoover, J. R. E.; Gallagher, G., Jr.; Faucette, L. F.; Mong, S. M.; Johnson, R. K. *Chem. Res. Toxicol.* **1988**, *1*, 258.
- Boyd, F. L.; Stewart, D.; Remers, W. A.; Barkley, M. D.; Hurley, L. H. *Biochemistry* **1990**, *29*, 2387.
- Thurston, D. E.; Morris, S. J.; Hartley, J. A. *Chem. Commun.* **1996**, 563.
- Wilson, S. C.; Howard, P. W.; Forrow, S. M.; Hartley, J. A.; Adams, L. J.; Jenkins, T. C.; Kelland, L. R.; Thurston, D. E. *J. Med. Chem.* **1999**, *42*, 4028.
- Reddy, B. S. P.; Damayanthi, Y.; Reddy, B. S. N.; Lown, W. J. *Anti-Cancer Drug Des.* **2000**, *15*, 225.
- Baraldi, P. G.; Balboni, G.; Cacciari, B.; Guiotto, A.; Manfredini, S.; Romagnoli, R.; Spalluto, G.; Thurston, D. E.; Howard, P. W.; Bianchi, N.; Rutigliano, C.; Mischiati, C.; Gambari, R. *J. Med. Chem.* **1999**, *42*, 5131.
- Zhou, Q.; Duan, W.; Simmons, D.; Shayo, Y.; Raymond, M. A.; Dorr, R. T.; Hurley, L. H. *J. Am. Chem. Soc.* **2001**, *123*, 4865.
- Thurston, D. E.; Bose, D. S.; Thompson, A. S.; Howard, P. W.; Leoni, A.; Croker, S. J.; Jenkins, T. C.; Neidle, S.; Hartley, J. A.; Hurley, L. H. *J. Org. Chem.* **1996**, *61*, 8141.
- Gregson, S. J.; Howard, P. W.; Hartley, J. A.; Brooks, N. A.; Adams, L. J.; Jenkins, T. C.; Kelland, L. R.; Thurston, D. E. *J. Med. Chem.* **2001**, *44*, 737.
- Gregson, S. J.; Howard, P. W.; Gullick, D. R.; Hamaguchi, A.; Corcoran, K. E.; Brooks, N. A.; Hartley, J. A.; Jenkins, T. C.; Patel, S.; Guille, M. J.; Thurston, D. E. *J. Med. Chem.* **2004**, *47*, 1161.
- Gregson, S. J.; Howard, P. W.; Corcoran, K. E.; Jenkins, T. C.; Kelland, L. R.; Thurston, D. E. *Bioorg. Med. Chem. Lett.* **2001**, *11*, 2859.
- Kamal, A.; Rao, M. V.; Laxman, N.; Ramesh, G.; Reddy, G. S. K. *Curr. Med. Chem.—Anti-Cancer Agents* **2002**, *2*, 215.
- Kamal, A.; Ramesh, G.; Laxman, N.; Ramulu, P.; Srinivas, O.; Neelima, K.; Kondapi, A. K.; Srinu, V. B.; Nagarajaram, H. A. *J. Med. Chem.* **2002**, *45*, 4679.
- Kamal, A.; Laxman, N.; Ramesh, G.; Srinivas, O.; Ramulu, P. *Bioorg. Med. Chem. Lett.* **2002**, *12*, 1917.
- Kamal, A.; Reddy, B. S. N.; Reddy, G. S. K.; Ramesh, G. *Bioorg. Med. Chem. Lett.* **2002**, *12*, 1933.
- Kamal, A.; Ramulu, P.; Srinivas, O.; Ramesh, G. *Bioorg. Med. Chem. Lett.* **2003**, *13*, 3417.
- Kamal, A.; Ramesh, G.; Ramulu, P.; Srinivas, O.; Rehana, T.; Sheelu, G. *Bioorg. Med. Chem. Lett.* **2003**, *13*, 3451.
- Kamal, A.; Ramesh, G.; Ramulu, P.; Srinivas, O.; Rehana, T.; Sheelu, G. *Bioorg. Med. Chem. Lett.* **2003**, *13*, 3517.
- Kamal, A.; Ramulu, P.; Srinivas, O.; Ramesh, G. *Bioorg. Med. Chem. Lett.* **2003**, *13*, 3955.
- Kamal, A.; Ramesh, G.; Srinivas, O.; Ramulu, P. *Bioorg. Med. Chem. Lett.* **2004**, *14*, 471.
- Kamal, A.; Srinivas, O.; Ramulu, P.; Ramesh, G.; Kumar, P. P. *Bioorg. Med. Chem. Lett.* **2004**, *14*, 4107.
- Jones, G. B.; Davey, C. L.; Jenkins, T. C.; Kamal, A.; Kneale, G. G.; Neidle, S.; Webster, G. D.; Thurston, D. E. *Anti-Cancer Drug Des.* **1990**, *5*, 249.
- Langely, D. R.; Thurston, D. E. *J. Org. Chem.* **1987**, *52*, 91.
- McConnaughie, A. W.; Jenkins, T. C. *J. Med. Chem.* **1995**, *38*, 3488.